Hindawi
Mathematical Problems in Engineering
Volume 2019, Article ID 5026316, 13 pages
https://doi.org/10.1155/2019/5026316

Research Article

Suppression of Current Fluctuations and the Brake Torque for PMSM Shutoff in Electric Vehicles

Ke Lu,[1,2] Yuan Zhu ,[1,2] Zhihong Wu,[1,2] and Mingkang Xiao[2]

[1]*Sino-German School for Postgraduate Studies, Tongji University, Shanghai 200092, China*
[2]*School of Automotive Studies, Tongji University, Shanghai 200092, China*

Correspondence should be addressed to Yuan Zhu; yuan.zhu@tongji.edu.cn

Received 7 May 2019; Accepted 10 August 2019; Published 2 September 2019

Academic Editor: Yongheng Yang

When a safety-related fault in the motor controller is detected, the torque output of the motor cannot be effectively shut off in time and an overcurrent occurs at the moment of switching. The advantages and disadvantages of the open circuit and active short-circuit methods are analyzed. Combining the advantages of these two operations, this paper proposes a new mixed voltage modulation method. It introduces a voltage modulation ratio that represents the duty cycle of the open circuit operation during a PWM period. This ratio is first set to a fixed value and gradually reduced to zero. The inverter is switched at a mixed operation and finally remains in the active short-circuit mode. The current can be quickly converged by a freewheeling diode of open circuit. After switching to active circuit, the brake torque is safety. The effectiveness of this shutoff method was verified by simulations and experiments. It shows that current fluctuations are suppressed and the torque output is also within a safety range. In addition, this shutoff method does not require any additional sensor information and is simple to implement.

1. Introduction

In order to solve the environmental problem caused by automobile exhaust emissions, vehicle manufacturers have spared no effort to develop new energy vehicles, especially electric vehicles [1]. And among the different motor types, permanent magnet synchronous motors (PMSMs), especially internal PMSMs, have been widely used in electric vehicles and hybrid vehicles, due to their high power density, high efficiency, and small size [2, 3], and the design and development of motor controllers for electric vehicles has also been extensively studied [4–9].

However, as the electrification of automobiles has become the main direction of automobile development, the so-called "sudden unintended acceleration" of electric vehicles has been reported frequently, and the safety of the electric vehicles has drawn more attention. Nowadays, most of the auto manufacturers have required their suppliers to develop motor control systems according to the functional safety standards for vehicles ISO 26262 [10], and related studies are reported in [11–13]. Wu studied the functional safety concept development for powertrains of hybrid vehicles and electric vehicles [11]. Christiaens presented functional safety concept of PMSM controller for vehicles based on the E-Gas architecture, and the implementation of the motor control system was monitored by an independent functional layer [12]. Li put forward an online torque monitoring method for the motor and pointed out that when a critical failure is detected, the shutoff path could be triggered to allow the motor to enter a safe state to ensure that the vehicle is controlled or does not cause harm to the occupants [13].

And in order to switch the motor into the safe state, two methods are commonly used, i.e., the open-circuit operation or active short-circuit (ASC) operation method [14–16]. The main drawback of the open circuit operation is that a strong brake torque will be generated when the motor operates at high speed, which may lead to rear collision accident [17, 18]. And for the active short-circuit operation, the main disadvantage is that the excessive current may occur when entering the safe state [17–21], which means that if this method is applied, the controller requires IGBTs

with higher current tolerance. It will not only increase the costs of the hardware but will also enlarge the size of the inverter.

There have been some studies comparing these two methods in fault diagnosis and IGBT protection. Bin analyzed more than 20 methods for open-circuit fault and 10 methods for short circuit [22]. The modified normalized DC current method was proved to be very effective in detecting faults with high resistivity to false alarms among the open-circuit fault methods [23, 24]; however, the open-circuit operation will not be used as a general shutoff method because it will output strong brake torque when the motor rotates at high speed, which will violate the requirement from safety side. In short-circuit operation, various IGBT fault failure detection and protection strategies have been studied during the last decade.

Rothenhagen pointed out that the induced voltage across the stray induction between the Kelvin emitter and the power emitter can be used to monitor the fault current. When failure occurred, a slower turnoff mechanism was trigged to control the fault current change rate di/dt [25]. Protection by two-step gate pulse was proposed to detect fault in the inverter, and the gate voltage was reduced from its normal value to a lower value. It kept the di/dt low and avoided interference issues [26]. In [27], IGBTs were slowly turned off using additional passive components in fault conditions. Either a high value gate resistance or a high value of external capacitor was switched in parallel with the IGBT gate input capacitance. However, most of the above-mentioned methods are hardware circuit-based, and algorithms-based researches are few.

In previous studies, the selection of shutoff methods was generally based on field experience or experimental results and there was no theoretical analysis and comparison of these two methods. In this paper, the motor current and torque output of these two shutoff methods will be compared and theoretically analyzed.

In addition, very few studies have been published in shutoff method studies for reducing current fluctuation. Bosch has proposed a patent method for suppressing the current generated in the ASC operation [28]. However, this method relied on the rotor position, and the position sensor might not be available when a critical fault happens. This paper proposes a new shutoff method with a special voltage modulation ratio. It shows that the current fluctuation can be suppressed and the torque output can be also switched off without the risk to damage the IGBTs; additionally, no additional sensor information is required.

This paper is organized as follows. In Section 2, the mathematical model of PMSMs is introduced. Section 3 derives the mathematical formula of the open-circuit operation and ASC and then analyzes and compares the advantages and disadvantages of these two methods. Section 4 introduces a special voltage modulation ratio and proposes a new shutoff method. Section 5 presents the simulation and experimental results of ASC operation and the proposed method. The effectiveness of the method is compared with the short-circuit method and verified by simulations and experiments. In Section 6, the paper is summarized.

2. Mathematical Mode of PMSMs

Two types of PMSMs are widely used in the automotive industry, i.e., the round rotor PMSMs and the salient-pole PMSMs. The salient-pole PMSMs model can be expressed as

$$\begin{bmatrix} \frac{di_d}{dt} \\ \frac{di_q}{dt} \end{bmatrix} = \begin{bmatrix} -\frac{R_s}{L_d} & \frac{\omega L_d}{L_d} \\ -\frac{\omega L_d}{L_q} & -\frac{R_s}{L_q} \end{bmatrix} \begin{bmatrix} i_d \\ i_q \end{bmatrix} + \begin{bmatrix} \frac{1}{L_d} & 0 \\ 0 & \frac{1}{L_q} \end{bmatrix} \begin{bmatrix} u_d \\ u_q - \omega\psi_f \end{bmatrix}, \quad (1)$$

where u_d and u_q are the stator voltage of d-axis and q-axis, respectively, i_d and i_q are the stator current of d-axis and q-axis, respectively, L_d and L_q are the inductance in d-axis and q-axis, respectively, R_s is the stator resistance, ω is the electrical angular velocity of the rotor and $\omega_m = \omega/p_n$ is the mechanical angular velocity of the rotor, p_n is the number of pole pairs of motor, and ψ_f represents the flux generated by the rotor permanent magnet.

The torque equation of salient-pole PMSMs is

$$T_e = 1.5p_n\left[\psi_f i_q + \left(L_d - L_q\right) i_d i_q\right]. \quad (2)$$

And the model of round rotor PMSMs can be expressed as

$$\begin{bmatrix} \frac{di_d}{dt} \\ \frac{di_q}{dt} \end{bmatrix} = \begin{bmatrix} -\frac{R_s}{L_s} & \omega \\ -\omega & -\frac{R_s}{L_s} \end{bmatrix} \begin{bmatrix} i_d \\ i_q \end{bmatrix} + \begin{bmatrix} \frac{1}{L_s} & 0 \\ 0 & \frac{1}{L_s} \end{bmatrix} \begin{bmatrix} u_d \\ u_q - \omega\psi_f \end{bmatrix}, \quad (3)$$

where L_s is the rotor inductance.

The torque equation of round rotor PMSMs is

$$T_e = 1.5p_n\psi_f i_q. \quad (4)$$

As shown in Figure 1, this paper adopts the field-oriented control (FOC) strategy. When a safety-related fault in a motor controller is detected, a separate programmable device is activated to output PWM signal and the motor can be reliably switched to a safety state. Two methods are commonly used to switch the motor into safe state, i.e., the open-circuit operation or ASC operation method. The open-circuit operation means turning off all IGBTs in the inverter shown in Figure 2. In this case, T1–T6 are all switched off and diodes D1–D6 are used for freewheeling; ASC operation means that by switching on T2, T4, and T6 and switching off T1, T3, and T5, three phases of the motor are short circuited via the low-side IGBTs.

3. Derivation and Comparison of Current and Torque Response in Open Circuit and Active Short Circuit

3.1. Analysis of Open-Circuit Current and Torque Response of PMSM. According to the inverter topology shown in Figure 1, in the open circuit operation, the IGBTs are switched off and the current is fed back to the DC power supply via the freewheeling diode. The conduction sequence of the diode in

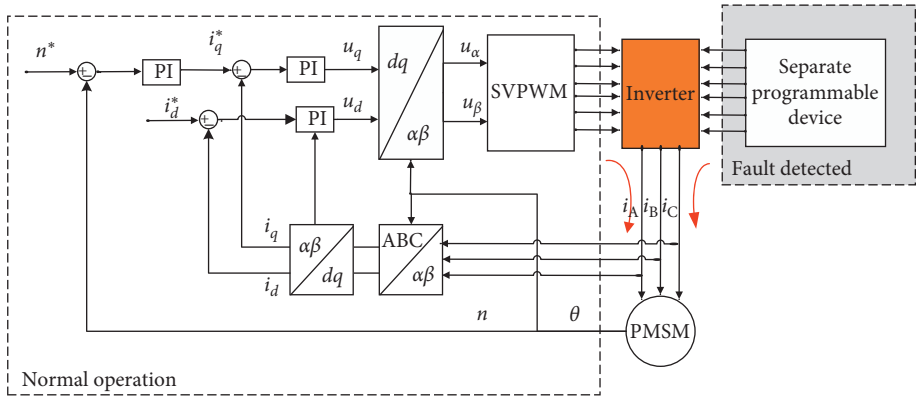

Figure 1: Control schematic diagram of PMSM.

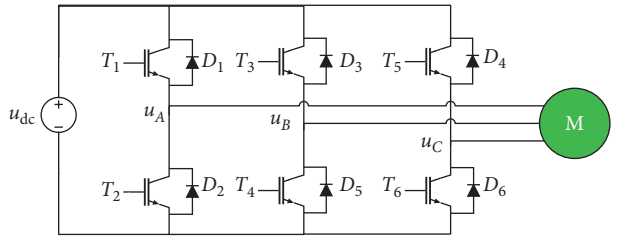

Figure 2: Topological structure of three-phase voltage type inverter.

this process mainly depends on the direction of the three-phase current of PMSMs. The voltages applied on the motor phases can be expressed as

$$\begin{bmatrix} u_a \\ u_b \\ u_c \end{bmatrix} = \begin{bmatrix} \dfrac{-\text{sign}(i_a)U_{dc}}{2} \\ \dfrac{-\text{sign}(i_b)U_{dc}}{2} \\ \dfrac{-\text{sign}(i_c)U_{dc}}{2} \end{bmatrix}, \tag{5}$$

where u_{dc} represents the bus voltage of PMSMs; u_a, u_b, and u_c are the three-phase voltage of PMSMs; and i_a, i_b, and i_c are the three-phase current of PMSMs.

In the open-circuit operation, u_a, u_b, and u_c can make up six basic voltage vectors and the magnitudes of these six voltage vectors are constant. The directions are directed to the 0°, 60°, 120°, 180°, 240°, and 300°, respectively, and are opposite to the directions of the sectors in which the motor current vectors are located.

According to equation (5), the input voltage of the motor is a nonlinear function of the motor current and the mathematical model of the motor itself is also a coupled system, so the solution to the time-domain response is very difficult to obtain. However, in the process of transition, the direction of voltage applied on the motor is always opposite to the direction of current, so the current can be quickly converged. After a short period of fluctuation, the current enters a stable state. In order to solve the steady-state current, the model of PMSM is simplified as follows:

(1) Only the fundamental component of the input voltage is under consideration

(2) The motor speed changes slowly and is regarded as a constant during analysis

In steady state, the three-phase current changes with sine and in the stationary coordinate system can be expressed as

$$\begin{bmatrix} i_\alpha \\ i_\beta \end{bmatrix} = \begin{bmatrix} i_s \cos\beta \\ i_s \sin\beta \end{bmatrix}, \tag{6}$$

where β is the stator current vector angle and i_s represents the current vector.i_α and i_β are the current in α-axis and β-axis, respectively.

The three-phase stator currents can be described as follows:

$$\begin{bmatrix} i_a \\ i_b \\ i_c \end{bmatrix} = \begin{bmatrix} i_s \cos\beta \\ i_s \cos\left(\beta - \dfrac{2\pi}{3}\right) \\ i_s \cos\left(\beta - \dfrac{4\pi}{3}\right) \end{bmatrix}. \tag{7}$$

According to equation (5), the three-phase voltages of the motor also change with the direction of the current. The three-phase voltages can be expressed as

$$\begin{bmatrix} u_a \\ u_b \\ u_c \end{bmatrix} = \begin{bmatrix} \begin{cases} \frac{U_{dc}}{2} & \text{if } \beta \in \left(\frac{\pi}{2}, \frac{3\pi}{2}\right) \\ -\frac{U_{dc}}{2} & \text{if } \beta \in \left(0, \frac{\pi}{2}\right) \vee \beta \in \left(\frac{3\pi}{2}, 2\pi\right) \end{cases} \\ \begin{cases} -\frac{U_{dc}}{2} & \text{if } \beta \in \left(\frac{\pi}{6}, \frac{7\pi}{6}\right) \\ \frac{U_{dc}}{2} & \text{if } \beta \in \left(0, \frac{\pi}{6}\right) \vee \beta \in \left(\frac{7\pi}{6}, 2\pi\right) \end{cases} \\ \begin{cases} -\frac{U_{dc}}{2} & \text{if } \beta \in \left(\frac{5\pi}{6}, \frac{11\pi}{6}\right) \\ \frac{U_{dc}}{2} & \text{if } \beta \in \left(0, \frac{5\pi}{6}\right) \vee \beta \in \left(\frac{11\pi}{6}, 2\pi\right) \end{cases} \end{bmatrix}. \quad (8)$$

According to the Clark transformation, the three-phase stator voltages in the stationary coordinate system can be calculated as follows:

$$\begin{bmatrix} u_\alpha \\ u_\beta \end{bmatrix} = \begin{bmatrix} \begin{cases} \frac{2U_{dc}}{3} & \text{if } \beta \in \left(\frac{5\pi}{6}, \frac{7\pi}{6}\right) \\ -\frac{2U_{dc}}{3} & \text{if } \beta \in \left(0, \frac{\pi}{6}\right) \vee \beta \in \left(\frac{11\pi}{6}, 2\pi\right) \\ -\frac{U_{dc}}{3} & \text{if } \beta \in \left(\frac{\pi}{6}, \frac{\pi}{2}\right) \vee \beta \in \left(\frac{3\pi}{2}, \frac{11\pi}{6}\right) \\ \frac{U_{dc}}{3} & \text{if } \beta \in \left(\frac{\pi}{2}, \frac{5\pi}{6}\right) \vee \beta \in \left(\frac{7\pi}{6}, \frac{3\pi}{2}\right) \end{cases} \\ \begin{cases} -\frac{\sqrt{3}U_{dc}}{3} & \text{if } \beta \in \left(\frac{\pi}{6}, \frac{5\pi}{6}\right) \\ \frac{\sqrt{3}U_{dc}}{3} & \text{if } \beta \in \left(\frac{7\pi}{6}, \frac{11\pi}{6}\right) \\ 0 & \text{if } \beta \in \left(0, \frac{\pi}{6}\right) \vee \beta \in \left(\frac{11\pi}{6}, 2\pi\right) \vee \beta \in \left(\frac{5\pi}{6}, \frac{7\pi}{6}\right) \end{cases} \end{bmatrix}. \quad (9)$$

For a motor in a star connection scheme, the even and third harmonics of the stator voltage cancel each other and it mainly includes the fundamental component, the 5th and 7th harmonics. To simplify the analysis, the remaining 5th and 7th harmonics are ignored. By performing the Fourier decomposition on the stator voltage in the stationary coordinate system according to equation (9), the fundamental component of the voltage can be expressed as

$$\begin{bmatrix} u_\alpha \\ u_\beta \end{bmatrix} = \begin{bmatrix} -\frac{2U_{dc}}{\pi}\cos\beta \\ -\frac{2U_{dc}}{\pi}\sin\beta \end{bmatrix}. \quad (10)$$

Also, it can be described as

$$\begin{bmatrix} u_\alpha \\ u_\beta \end{bmatrix} = \begin{bmatrix} \frac{2U_{dc}}{\pi}\cos(\beta+\pi) \\ \frac{2U_{dc}}{\pi}\sin(\beta+\pi) \end{bmatrix}. \quad (11)$$

It can be seen that under steady-state conditions, the fundamental component of the stator voltage has a constant amplitude. By comparing equation (6) with equation (11), the direction of the voltage vector is opposite to the direction of the steady-state current vector. Simultaneously, the voltage vector rotates with the rotor coordinate system, so the steady-state current response can be obtained using a vector diagram. The round rotor PMSMs and the salient-pole PMSMs will be analyzed, respectively.

3.1.1. Round Rotor PMSMs. If only the fundamental component of the input voltage is considered, from equation (3), the vector diagram of the round rotor PMSM is shown in Figure 3.

And according to Figure 3, the corresponding trigonometric equation can be established:

$$\begin{cases} -\frac{u_s i_q}{\sqrt{i_d^2 + i_q^2}} = R_s i_q + \omega\psi_f + \omega L_s i_d, \\ -\frac{u_s i_d}{\sqrt{i_d^2 + i_q^2}} = R_s i_d - \omega L_s i_q. \end{cases} \quad (12)$$

By solving equation (12), the steady current response in the open circuit operation can be obtained. The root depends on the electrical angular speed and the turning speed can be calculated as follows:

$$\omega^* = \sqrt{\frac{4U_{dc}^2}{\pi^2\psi_f^2} - \frac{R_s^2}{L_s^2}}. \quad (13)$$

Since R_s is small and R_s/L_s is close to 0, it can be ignored. Thus, equation (13) can be simplified as

$$\omega^* = \frac{2U_{dc}}{\pi\psi_f}. \quad (14)$$

Equation (12) does not have a real number solution when the electrical angular speed is lower than the turning speed. In that case, the diode of the inverter maintains the voltage balance by switching the conduction direction and the motor current response is close to zero. When the electrical angular speed is greater than the turning speed ω^*, the steady-state response of the motor current is

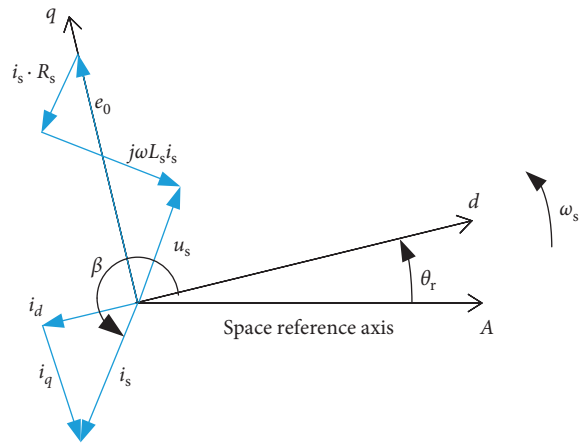

Figure 3: Vector diagram of the round rotor PMSM in open-circuit operation.

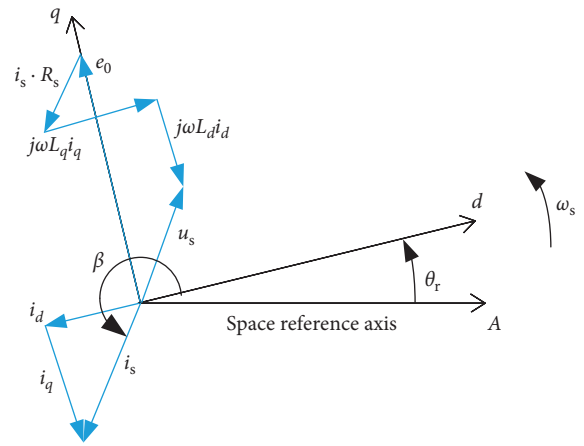

Figure 4: Vector diagram of salient-pole PMSM in open circuit operation.

$$i_d = \frac{4U_{dc}^2}{\pi^2 \psi_f L_s \omega^2} - \frac{\psi_f}{L_s}, \tag{15}$$

$$i_q = -\frac{2U_{dc}\sqrt{\omega^2 - \left(4U_{dc}^2/\pi^2\psi_f^2\right)}}{\pi L_s \omega^2}. \tag{16}$$

Below the turning speed, since the current response is 0, the torque output of the motor is also equal to 0. Above turning speed ω^*, according to equations (4) and (16), the electromagnetic torque can be calculated as follows:

$$T_e = -\frac{3\psi_f U_{dc} p_n \sqrt{\omega^2 - \left(4U_{dc}^2/\pi^2\psi_f^2\right)}}{\pi L_s \omega^2}. \tag{17}$$

3.1.2. Salient-Pole PMSMs. Similar to the analysis of round rotor PMSMs, salient-pole PMSMs in the open circuit are analyzed as follows. The vector diagram is shown in Figure 4:

According to the trigonometric function relationship, a function of the current can be obtained as follows:

$$\begin{cases} -\dfrac{u_s i_q}{\sqrt{i_d^2 + i_q^2}} = R_s i_q + \omega\psi_f + \omega L_d i_d, \\ -\dfrac{u_s i_d}{\sqrt{i_d^2 + i_q^2}} = R_s i_d - \omega L_q i_q. \end{cases} \tag{18}$$

Although the analytical solution of equation (18) cannot be directly obtained, it can be quantitatively analyzed and solved by numerical methods. From Figure 3, it can be seen that the vector relationship can be established when the rotation speed is sufficiently high, i.e., the back electromotive force is sufficiently large. This means that for a salient-pole motor, there is also a turning speed. Below the turning speed, the current response of the motor is approximately 0. When the speed is higher than the turning speed, the steady-state current of the d-q axis is negative in order to satisfy the vector relationship, which means that the torque output of the motor is also negative.

Therefore, a simulation was made to obtain the brake torque at different mechanical speed in the open-circuit operation. The result is shown in Figure 5. It can be seen that when the speed is higher than turning speed, the brake torque increases rapidly to a large value. In this case, brake torque occurs when the motor is operating at a high speed, which is extremely dangerous for the electrical vehicle.

Based on the analysis of round rotor PMSM and salient-pole PMSM in open-circuit operation, it can be seen as follows:

(1) The motor speed has a great influence on the current and torque responses of the motor. At low speeds (below the turning speed), the steady-state response of the current of d-axis and q-axis is zero and the motor has no torque output. At high speeds (above the turning speed), the steady-state response of the current of d-axis and q-axis is less than zero and the motor outputs brake torque.

(2) In the transient state of the current, the direction of voltage applied on the motor is always opposite to the direction of current, so the convergence of the current can be accelerated and the motor can quickly enter to a steady state.

(3) When the motor rotates above the turning speed, large brake will occur, which violates the safety requirements.

3.2. Analysis of Active Short-Circuit Current Response and Torque Response of PMSM. After switching into ASC state, the motor inputs u_d and u_q become 0. By solving equation (1), the current response in salient-pole PMSMs can be calculated as

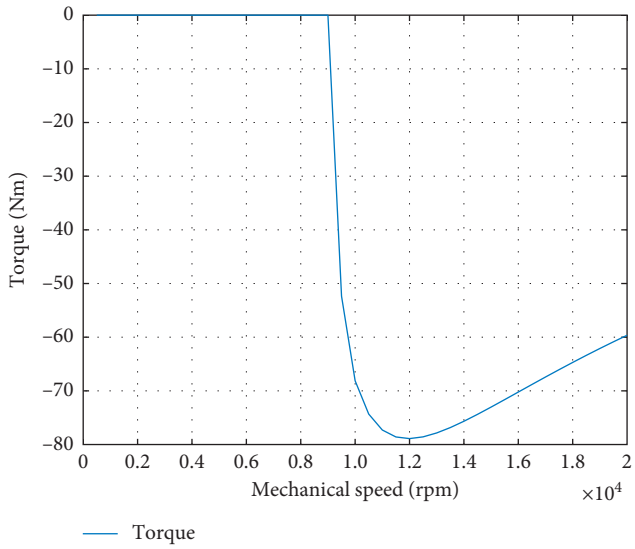

Figure 5: Brake torque in open-circuit operation in simulation (the PMSM parameters used in this simulation include the inductance in d-axis and q-axis $L_d = 0.1425$ mH and $L_q = 0.3359$ mH, the stator phase resistance $R_s = 0.016\,\Omega$, the flux generated by the rotor permanent magnet $\psi_f = 0.0566$ Wb, and the pole pairs $p_n = 4$).

$$i(t) \approx \begin{pmatrix} \dfrac{\left(L_d \widehat{i}_{d0} \cos(\omega t) + L_q \widehat{i}_{q0} \sin(\omega t)\right)}{L_d} e^{-\left(R_s t \left(L_d + L_q\right)/2 L_d L_q\right)} \\ \dfrac{\left(L_q \widehat{i}_{q0} \cos(\omega t) - L_d \widehat{i}_{d0} \sin(\omega t)\right)}{L_q} e^{-\left(R_s t \left(L_d + L_q\right)/2 L_d L_q\right)} \end{pmatrix} + \begin{pmatrix} -\dfrac{\omega^2 L_q \psi_f}{\left(L_d L_q \omega^2 + R_s^2\right)} \\ -\dfrac{\omega R_s \psi_f}{\left(L_d L_q \omega^2 + R_s^2\right)} \end{pmatrix}, \tag{19}$$

where $\widehat{i}_{d0}$ and $\widehat{i}_{q0}$ are the initial auxiliary variable of d-axis and q-axis and can be expressed as

$$\begin{aligned} \widehat{i}_{d0} &= i_d(0) - \left(-\frac{\omega^2 L_q \psi_f}{\left(L_d L_q \omega^2 + R_s^2\right)}\right), \\ \widehat{i}_{q0} &= i_q(0) - \left(-\frac{\omega R_s \psi_f}{\left(L_d L_q \omega^2 + R_s^2\right)}\right). \end{aligned} \tag{20}$$

According to equation (19), the current response of the d-q axis is composed of a steady-state response and a transient-state response. Transient response is related to current fluctuation in transition process. In the transient part of the current, the transient current is gradually convergent in an elliptic spiral curve in the d-q coordinate system. According to equation (21), the fluctuation magnitude of the transient current amplitude $A(t)$ mainly depends on the inductance of the motor and initial current at the moment of entering ASC, i.e., $\widehat{i}_{d0}$ and $\widehat{i}_{q0}$. Since the inductance of the motor is not big enough, $\widehat{i}_{d0}$ and $\widehat{i}_{q0}$ are the main factors. Equation (20) indicates that $\widehat{i}_{d0}$ and $\widehat{i}_{q0}$ represent the difference between the initial current at the moment of entering ASC and the steady-state current. The closer the initial current and steady-state current are, the smaller the amplitude of the fluctuation is.

$$\begin{aligned} A(t) &= \frac{L_d \widehat{i}_{d0} \cos(\omega t) + L_q \widehat{i}_{q0} \sin(\omega t)}{L_d} \\ &= \sqrt{\widehat{i}_{d0}^2 + \left(\frac{L_q}{L_d} \widehat{i}_{q0}\right)^2} \sin(\omega t + \varphi), \end{aligned} \tag{21}$$

where φ can be expressed as $\varphi = \arctan\left(L_d \widehat{i}_{d0} / L_q \widehat{i}_{q0}\right)$.

By substituting the steady-state current response into the torque equation (2), the torque output of the motor can also be obtained:

$$T_e = -1.5 p_n \left(\frac{\omega_e R_s \psi_f^2}{L_d L_q \omega_e^2 + R_s^2} - \frac{\omega_e^3 L_q R_s \psi_f^2 \left(L_d - L_q\right)}{\left(L_d L_q \omega_e^2 + R_s^2\right)^2}\right). \tag{22}$$

It can be seen from equation (22) that the motor speed has a significant influence on the torque: when the motor speed is high ($L_d L_q \omega^2 \gg R_s^2$), the motor torque equation can be simplified as:

$$T_e = -1.5 p_n \left(\frac{R_s \psi_f^2}{L_d L_q \omega} - \frac{R_s \psi_f^2 \left(L_d - L_q\right)}{L_d^2 L_q \omega}\right). \tag{23}$$

Equation (23) indicates that the output torque of the motor is inversely proportional to the rotation speed. The higher the rotation speed is, the smaller the torque output is. As the motor speed gradually decreases, the brake torque gradually increases.

In the case of a very low speed ($\omega \ll \sqrt{R_s^2 / L_d L_q}$), the torque equation can be expressed as

$$T_e = -1.5 p_n \left(\frac{\omega \psi_f^2}{R_s} - \frac{\omega^3 L_q \psi_f^2 \left(L_d - L_q\right)}{R_s^3}\right). \tag{24}$$

As shown in Figure 6, a simulation is made to study the relationship between the mechanical speed and the brake torque. It can be seen that only at extremely low speed, the torque response is obvious, but the speed is very low at this time and it has little possibility to cause damage. In a wider speed range, the brake torque is close to 0 in the ASC mode. Thus, this torque output method is safe.

Since the inductance in d-axis is same as in q-axis, the analysis in round rotor PMSM is similar to in salient-pole PMSM.

Based on the analysis above, it can be concluded that

(1) In a wide mechanical speed range, the brake torque is close to 0. Only at extremely low speed, the torque response is obvious, but the speed is very low at this time and it has little possibility to cause damage.

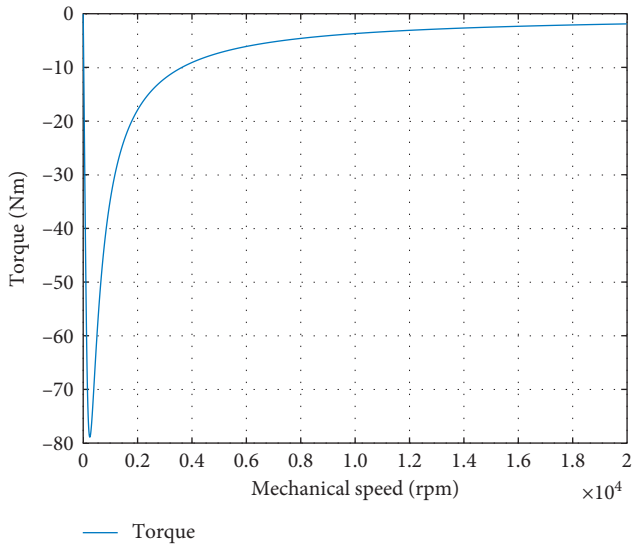

Figure 6: Brake torque in active short-circuit operation in simulation (the PMSM parameters used in this simulation include the inductance in d-axis and q-axis $L_d = 0.1425$ mH and $L_q = 0.3359$ mH, the stator phase resistance $R_s = 0.016\,\Omega$, the flux generated by the rotor permanent magnet $\psi_f = 0.0566$ Wb, and the pole pairs $p_n = 4$).

(2) Large transient current will be generated at the moment of switching. The amplitude of transient current mainly depends on the difference of initial current at the moment of entering ASC and the steady-state current. The smaller the difference is, the smaller the amplitude of the fluctuation is.

4. A New Shutoff Method of Suppressing Transient Current and Brake Torque

Although ASC can be used as a general shutoff method because it will not violate the requirement from safety side, the transient current caused at the instant of switching may exceed the maximum current that the IGBT can withstand, resulting in a shortened lifecycle or even direct burnout of the device.

From the analysis results of equations (20) and (21), it can be found that the magnitude of the transient fluctuation of the short-circuit current is related to the current at the moment the short circuit is activated. The closer the initial current and steady-state current are, the smaller the amplitude of the fluctuation is. If possible, control the current close to the stable current of short-circuit operation in advance and then switch to ASC operation. So in this way, the transient current in ASC can be suppressed. Afterwards, because the brake torque is close to 0 in a large range of speed in ASC operation, the motor can not only generate smaller transient current fluctuation but also output safety brake torque.

According to the analysis in the open-circuit mode, it can accelerate the convergence of transient current. This advantage can be used to keep the initial current quickly close to the steady-state current in order to suppress the fluctuation of transient current in ASC. Therefore, a special voltage modulation method is proposed in this paper. Before switching into ASC operation, this special voltage modulation operation is switched on.

In this method, a special voltage modulation ratio is introduced as follows:

$$M = \frac{T_{FW}}{T_{FW} + T_{ASC}}, \tag{25}$$

where T_{FW} and T_{ASC} represent time in open-circuit and in short-circuit operation, respectively.

This special modulation method can be regarded as a mixture of "open-circuit" and "short-circuit" operation. In this case, the voltage equation on the motor can be expressed as

$$\vec{u}_s = (1 - M)\vec{u}_{ASC} + M\vec{u}_{FW}. \tag{26}$$

When $M = 0$, PMSMs operate in the short-circuit mode. When $M = 1$, PMSMs operate in the open-circuit mode. When $0 < M < 1$, PMSMs rotate in the mixture of "open-circuit" and "short-circuit" operation.

In this proposed method, IGBT drive signal waveform is shown in Figure 7, i.e., by turning off the upper bridges (or lower bridges) and switching on lower bridges (or upper bridges) in a PWM manner.

Similar response analysis as the open-circuit operation can be applied. Stable current responses with different duty cycles are shown in Figure 8. As can be seen, the smaller the duty cycle is, the closer the steady-state current of the proposed method to the steady-state current of ASC operation is. Therefore, in the proposed shutoff operation, the ratio of the open- and short-circuit time is first set to a fixed value. The purpose is to allow the current to quickly converge to a value close to the short-circuit steady-state current and the duty cycle of open-circuit operation is gradually reduced to switch the inverter to the ASC mode smoothly and finally the motor state remains in ASC.

Another benefit of this approach is that it does not rely on any additional sensors. As long as the duty cycle is set, the current suppression can be achieved. In case of a serious error in the motor controller unit (MCU), a separate programmable device is activated to realize PWM output.

5. Simulation and Experiment Verification

5.1. Experimental Setup. Simulations and experiments were conducted to verify the effectiveness of the proposed method. The experimental platform shown in Figure 9 includes the tested PMSM, a load motor, a MCU, two personal computers (PCs), a signal conversion device (Kvaser), a data collection device (Vector VX1060), a speed sensor, and a torque sensor. MCU contains a controller and an inverter. The core of the control board is an Infineon digital signal microprocessor (Infineon TC1782). Two PCs are used in this experiment. The first one is used to control the load motor, which provides various load torques for PMSM. The second one sends out CAN control signal to MCU, which will also collect data through VX1060 and then feed back to the second PC.

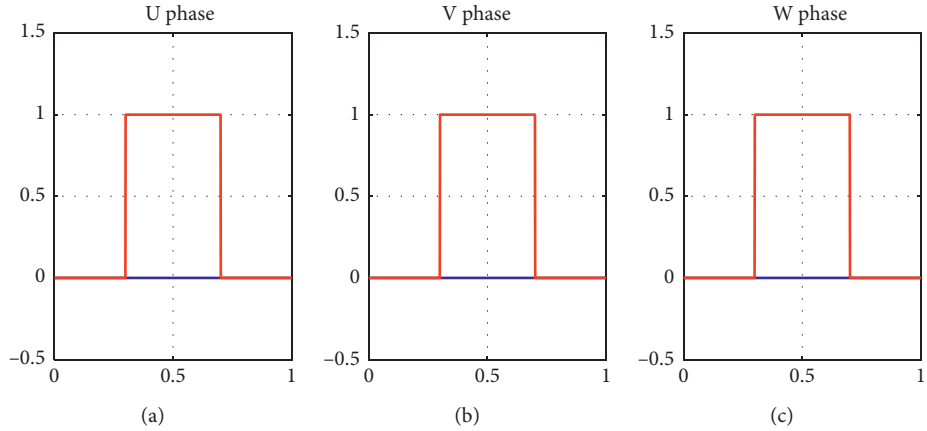

Figure 7: IGBT drive signal waveform: upper bridges (blue) and lower bridges (red).

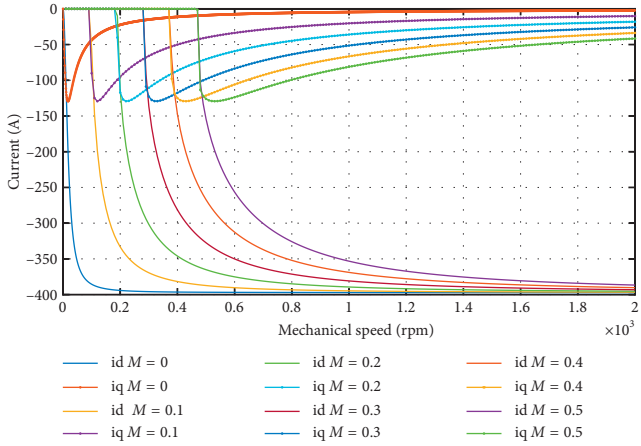

Figure 8: Steady-state current at different voltage modulation ratios (the PMSM parameters used in this simulation include the inductance in d-axis and q-axis $L_d = 0.1425$ mH and $L_q = 0.3359$ mH, the stator phase resistance $R_s = 0.016\,\Omega$, the flux generated by the rotor permanent magnet $\psi_f = 0.0566$ Wb, pole pairs $p_n = 4$).

The PMSM parameters used in this simulation include the output power $P_e = 45$ KW, rated voltage $U_e = 330$ V, rated speed $n_e = 3300$ rpm, the inductance in d-axis and q-axis $L_d = 0.1425$ mH and $L_q = 0.3359$ mH, the stator phase resistance $R_s = 0.016\,\Omega$, the flux generated by the rotor permanent magnet $\psi_f = 0.0566$ Wb, and pole pairs $p_n = 4$.

The motor speed is set at 1000 rpm, 3000 rpm, and 5000 rpm, respectively, and the current and torque responses in ASC and the proposed method are analyzed and compared both in simulations and experiments. The motor output torque before switching is 50 Nm. In the proposed method, the PWM period is 100 μs and duty cycle, i.e., the voltage modulation ratio, is initially set to 40% and reduced by 0.4% in every PWM cycle until it reaches 0.

5.2. Current Fluctuation Suppression. Figures 10–12 show the current response of ASC and the proposed method at three different speeds. Simulation and experiment results are compared and analyzed as follows.

In the experiment, it can be seen from Figure 12(a) that in the proposed method, the current in d-axis can drop rapidly to a steady-state current and fluctuate slightly within 0.002 s. Compared with the ASC strategy, the maximum amplitude is less than 500 A and the current amplitude is reduced by 46%. Figure 12(b) also shows that the current in q-axis first decreases and then rapidly gets close to the steady-state current within 0.01 s, while under the traditional ASC operation, the current fluctuates greatly and the amplitude is large until it reaches the steady-state current at 0.04 s. Similarly, the suppression effect using the proposed method at 3000 rpm is also obvious. The current ripple is significantly reduced compared to systems in ASC mode. From Figure 11(a), the amplitude of the q-axis current is reduced from 853.7 A to 509.2 A. Although the current in q-axis indicates a large drop at the instance of switching, which is still 60 A smaller than the ASC method, it can rapidly reach the steady state and the fluctuation amplitude is limited to 50 A. Figures 10(a) and 10(b) show that there are also some suppression effects at 1000 rpm.

Figures 13 and 14 show a comparison of current amplitude responses at different speeds. The orange and the red lines indicate that the current amplitudes of d-axis and q-axis are small. The difference in amplitude between the proposed method and ASC is large at high speeds, which means that the suppression effect is better at high speeds.

In addition, the proposed method can speed up the convergence. Figure 11 shows at 5000 rpm, this method can approach the steady-state current of ASC in just 0.01 s, while the ASC time lasts 0.05 s. As can be seen from Figures 9 and 10, the proposed method can achieve a better convergence performance than ASC at two other different speeds.

The experimental verification is consistent with the simulation results. However, according to the waveform, a difference in steady-state current can be observed, which is caused by a change in parameters during motor operation. This difference is not large enough, and the experiment results of the proposed method can satisfy the safety requirements.

Theoretically, the open-circuit mode takes up a large duty circle at the beginning of shutoff process. Since the

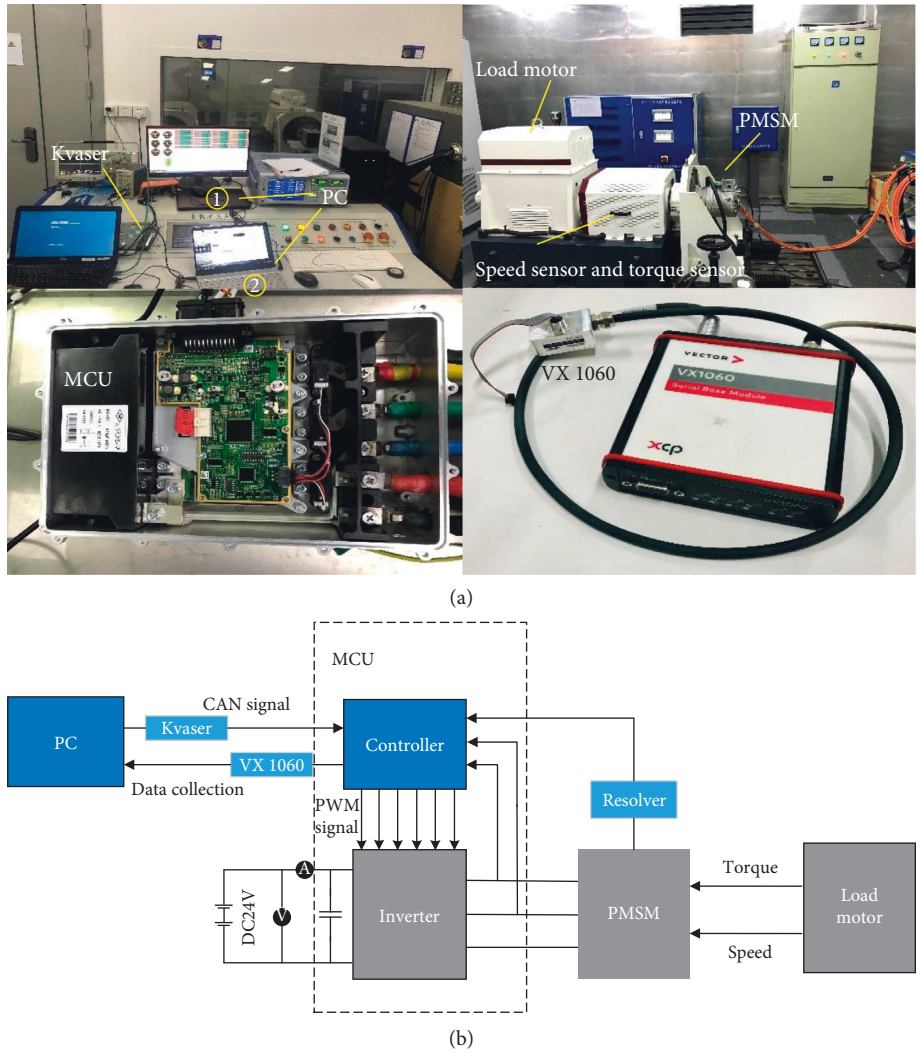

Figure 9: PMSM test platform: (a) experimental platform; (b) block diagram of test platform.

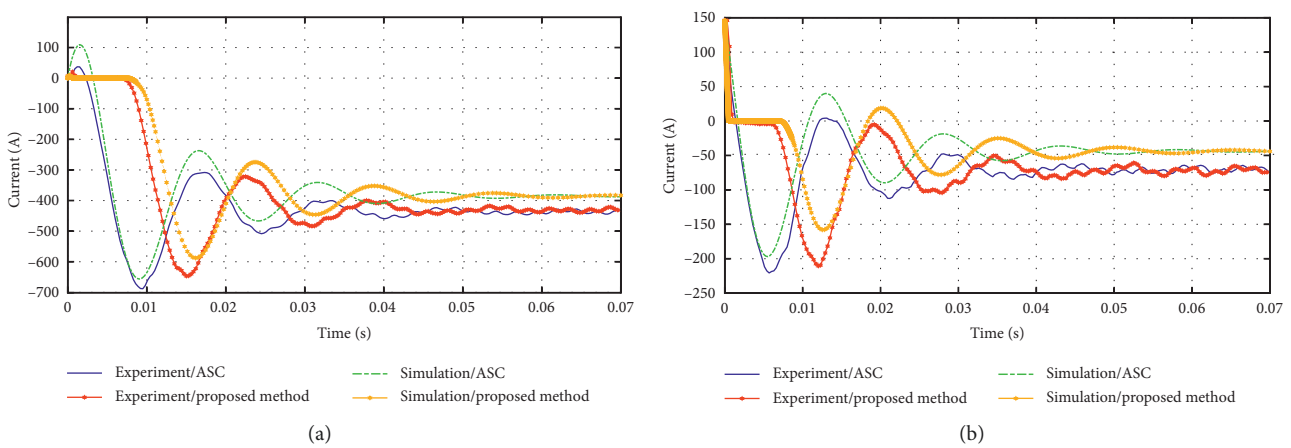

Figure 10: Current response at 1000 rpm: (a) d-axis and (b) q-axis.

voltage vector and current vector are in opposite directions, the excessive current can be quickly and effectively suppressed. To sum up, experiments verify the effectiveness of the proposed method in restraining current amplitude and accelerating convergence speed, which is consistent with theoretical analysis.

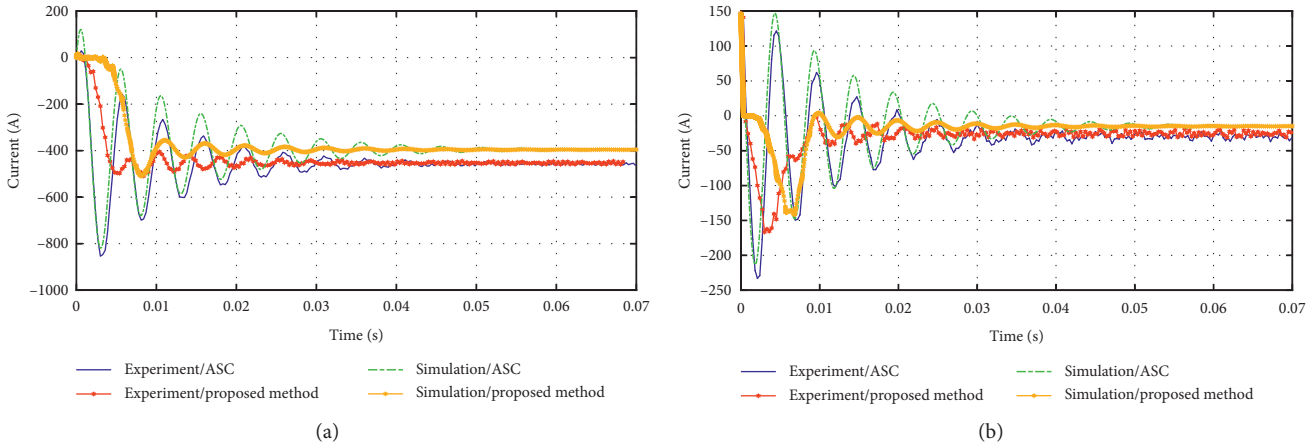

Figure 11: Current response at 3000 rpm: (a) d-axis and (b) q-axis.

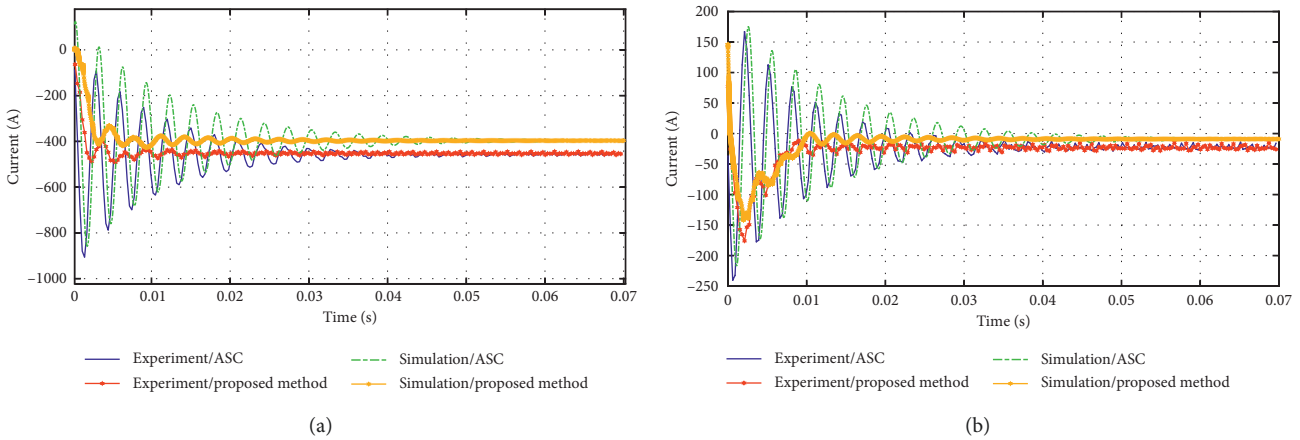

Figure 12: Current response at 5000 rpm: (a) d-axis and (b) q-axis.

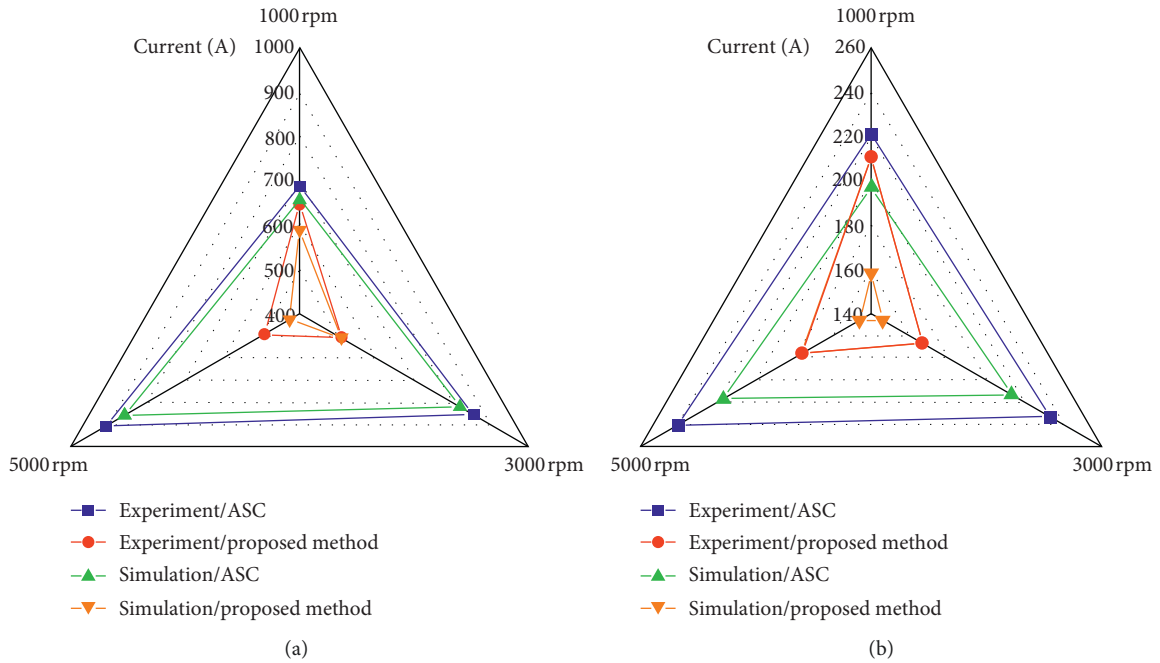

Figure 13: Comparison of amplitude of current response at different speeds: (a) d-axis and (b) q-axis.

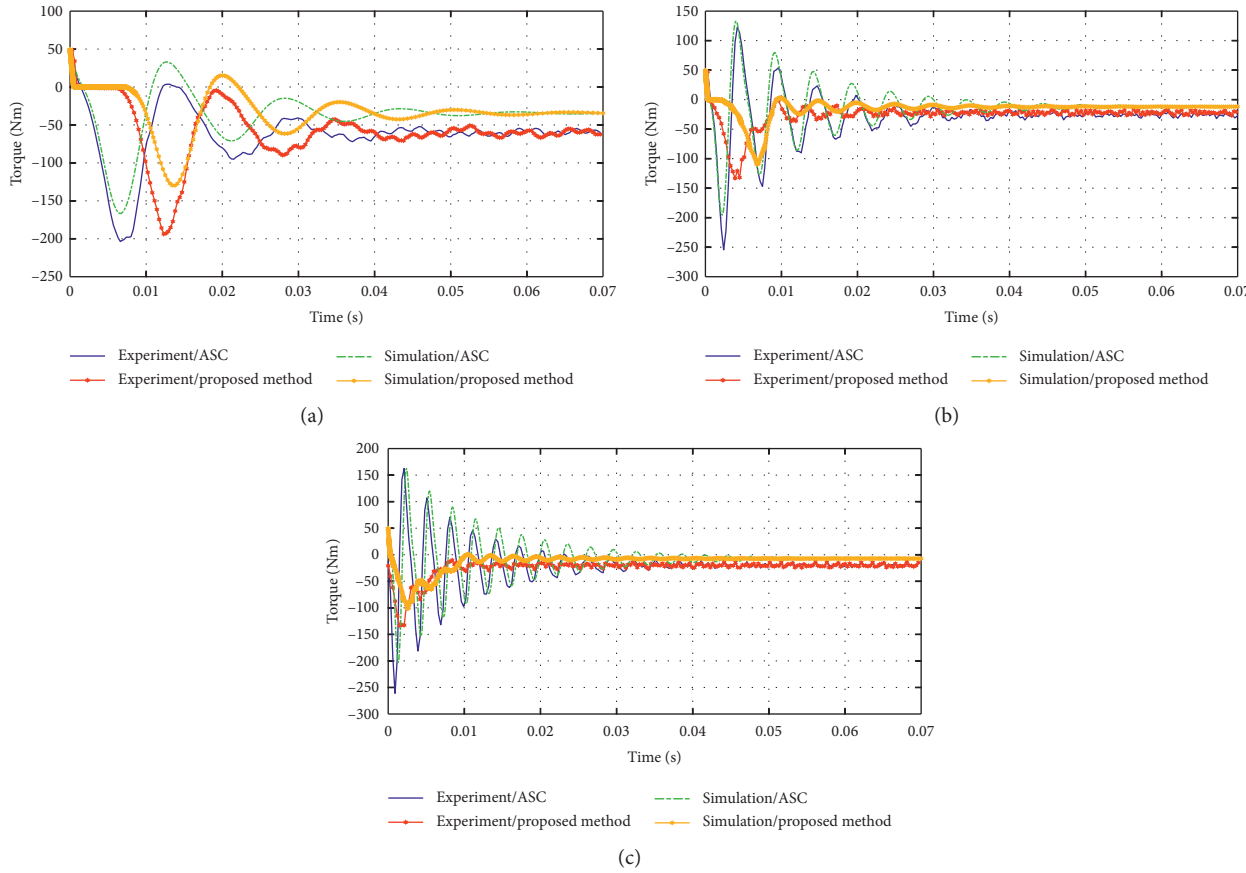

Figure 14: Torque response at different speeds: (a) 1000 rpm; (b) 3000 rpm; (c) 5000 rpm.

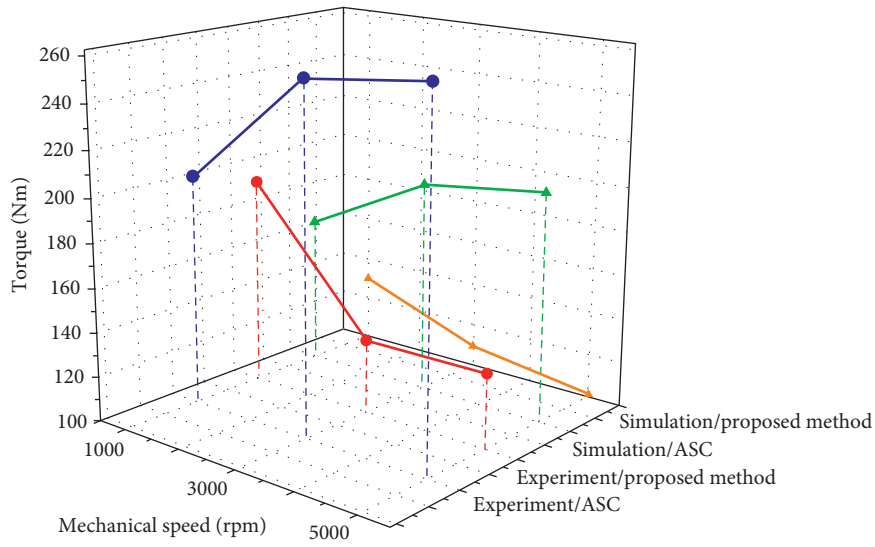

Figure 15: Comparison of brake torque amplitude at different speeds.

5.3. Brake Torque Suppression. Figure 14 shows the response of brake torque using the proposed method and ASC at three different speeds.

From Figures 14(b) and 14(c), it shows that at 3000 rpm and 5000 rpm, when the system is stable, the stable brake torque is close to 0, indicating that the motor torque can be effectively cut off under both the ASC and the proposed method. Although the steady-state brake torque at 1000 rpm is close to 50 Nm, which is shown in Figure 14(a), this torque will not cause harm to the PMSM because the speed is not

fast enough. Therefore, the proposed method can also output safe brake torque without violating safety requirements.

Figure 15 shows a comparison of brake torque amplitudes at different speeds. The red and orange lines represent the amplitude of brake torque under the proposed operation, which is less than the amplitude of ASC shown in blue and green lines. At 5000 rpm, the torque is reduced from 261 Nm to 133 Nm experimentally, and the amplitude at 3000 rpm is also 120 Nm less than in ASC. The smaller the amplitude of brake torque at the instance of switching is, the higher the degree of safety is.

Moreover, from Figure 14(a), at 1000 rpm, the proposed method indicates the same convergence rate as the ASC. However, as can be seen in Figures 14(b) and 14(c), it takes only 0.02 s (at 3000 rpm) or 0.01 s (at 5000 rpm) to suppress the brake torque close to 0, while the convergence time lasts 0.04 s under the ASC mode, which means the proposed method can accelerate the convergence at high speed. It can be seen that, as the speed increases, the convergence effect will also be improved.

The experiment verification is in agreement with the simulation results. The improvement is reflected in the smaller brake torque amplitude and faster convergence speed.

6. Conclusions

This paper focuses on the shutoff methods commonly used in the functional safety development of PMSM controllers for electric vehicles, i.e., open-circuit operation and ASC operation.

The open-circuit operation will not be switched as a general shutoff method due to the large brake torque output above turning speed. For the ASC mode, large excessive currents will exceed the maximum limit that IGBT can withstand, which will damage the IGBT and shorten the lifecycle of the inverter. In order to improve the reliability of the inverter, IGBTs with large current capacity and high quality are selected, which will increase the cost of the device. The method proposed in this paper can suppress the excessive current fluctuation and accelerate the convergence by introducing a special voltage modulation ratio. As the speed increases, the suppression effect is verified to be better. Furthermore, the proposed method is more effective in decreasing the amplitude of brake torque and increasing the convergence speed at high speed compared to the ASC. In addition, this proposed shutoff mode does not require any additional sensor information and it is simple and easy to implement. This paper provides a theoretical basis and an implementation scheme for the proposed method. The effectiveness of proposed method is verified both in simulations and experiments.

In applications, improving the reliability and reducing the cost of IGBTs is the core issue in regarding new energy vehicles. The sudden burnout of IGBTs will result in failure of MCU, and the high cost of IGBTs will increase the cost of whole vehicle, which will slow down the industrialization of the electric vehicle. The optimization method proposed in this paper performs well in the protection of IGBTs and inverters through suppressing overcurrent fluctuations. IGBTs in inverters are also widely used in other fields of electric traction, for example, in railway traction. Therefore, the reliability and low cost of IGBTs play an important role in development of these industries. Future research will aim to find more effective suppression strategies at low speeds and extend the range of optimizations that can suppress the excessive current and brake torque.

Data Availability

The simulation and experimental data used to support the findings of this study are available from the corresponding author upon request.

Conflicts of Interest

The authors declare that there are no conflicts of interest.

Acknowledgments

This research was funded by the National Key Research and Development Program of China (2016YFB0100804).

References

[1] M. R. Mehrjou, N. Mariun, N. Misron, M. A. M. Radzi, and S. Musa, "Broken rotor bar detection in LS-PMSM based on startup current analysis using wavelet entropy features," *Applied Sciences*, vol. 7, no. 8, p. 845, 2017.

[2] G. Pellegrino, A. Vagati, P. Guglielmi, and B. Boazzo, "Performance comparison between surface-mounted and interior PM motor drives for electric vehicle application," *IEEE Transactions on Industrial Electronics*, vol. 59, no. 2, pp. 803–811, 2011.

[3] G. Pellegrino, A. Vagati, B. Boazzo, and P. Guglielmi, "Comparison of induction and PM synchronous motor drives for EV application including design examples," *IEEE Transactions on Industry Applications*, vol. 48, no. 6, pp. 2322–2332, 2012.

[4] K.-T. Nam, H. Kim, S.-J. Lee, and T.-Y. Kuc, "Observer-based rejection of cogging torque disturbance for permanent magnet motors," *Applied Sciences*, vol. 7, no. 9, p. 867, 2017.

[5] S. K. Kommuri, M. Defoort, H. R. Karimi, and K. C. Veluvolu, "A robust observer-based sensor fault-tolerant control for PMSM in electric vehicles," *IEEE Transactions on Industrial Electronics*, vol. 63, no. 12, pp. 7671–7681, 2016.

[6] X. Liu, H. Chen, J. Zhao, and A. Belahcen, "Research on the performances and parameters of interior PMSM used for electric vehicles," *IEEE Transactions on Industrial Electronics*, vol. 63, no. 6, pp. 3533–3545, 2016.

[7] Y. Miyama, M. Hazeyama, S. Hanioka, N. Watanabe, A. Daikoku, and M. Inoue, "PWM carrier harmonic iron loss reduction technique of permanent-magnet motors for electric vehicles," *IEEE Transactions on Industry Applications*, vol. 52, no. 4, pp. 2865–2871, 2016.

[8] H. Liang, Y. Chen, S. Liang, and C. Wang, "Fault detection of stator inter-turn short-circuit in PMSM on stator current and vibration signal," *Applied Sciences*, vol. 8, no. 9, p. 1677, 2018.

[9] K. Pietrusewicz, P. Waszczuk, and M. Kubicki, "MFC/IMC control algorithm for reduction of load torque disturbance in PMSM servo drive systems," *Applied Sciences*, vol. 9, no. 1, p. 86, 2018.

[10] International Organization for Standardization, *Road Vehicles—Functional Safety*, International Organization for Standardization, Geneva, Switzerland, 1st edition, 2011.

[11] Z. Wu, K. Lu, and Y. Zhu, "Functional safety and secure CAN in motor control system design for electric vehicles," in *Proceedings of the SAE World Congress Experience, WCX 2017*, Detroit, MI, USA, April 2017.

[12] S. Christiaens, J. Ogrzewalla, and S. Pischinger, "Functional safety for hybrid and electric vehicles," in *Proceedings of the SAE 2012 World Congress and Exhibition*, Detroit, MI, USA, April 2012.

[13] S. Li, C. Chang, and H. Zhao, "Functional safety development of E-motor drive system for PHEV," in *Proceedings of the SAE 2015 World Congress and Exhibition*, Detroit, MI, USA, April 2015.

[14] E. Pazoukiund, J. A. De Abreu-Garcia, and Y. Sozer, "Fault tolerant control method for interleaved DC-DC converters under open and short circuit switch faults," in *Proceedings of the 2017 IEEE Energy Conversion Congress and Exposition*, Cincinnati, OH, USA, October 2017.

[15] C.-J. Bae, S.-M. Lee, and D.-C. Lee, "Diagnosis of multiple IGBT open-circuit faults for three-phase PWM inverters," in *Proceedings of the 2016 IEEE 8th International Power Electronics and Motion Control Conference (IPEMC-ECCE Asia)*, Hefei, China, May, 2016.

[16] B. Sen and J. Wang, "Stationary frame fault-tolerant current control of polyphase permanent magnet machines under open-circuit and short-circuit faults," *IEEE Transactions on Power Electronics*, vol. 31, p. 4684, 2015.

[17] J. Fuhrmann, S. Klauke, and H.-G. Eckel, "IGBT and diode behavior during short-circuit type 3," *IEEE Transactions on Electron Devices*, vol. 62, no. 11, pp. 3786–3791, 2015.

[18] A. Virdag, T. Hager, J. Hu, and R. De Doncker, "Short circuit behavior of dual active bridge DCDC converter with low resistance DC side fault," in *Proceedings of the 2017 IEEE 8th International Symposium on Power Electronics for Distributed Generation Systems (PEDG)*, Florianopolis, Brazil, April, 2017.

[19] J. Hu, Z. He, L. Lin, K. Xu, and Y. Qiu, "Voltage polarity reversing-based DC short circuit FRT strategy for symmetrical bipolar FBSM-MMC HVDC system," *IEEE Journal of Emerging and Selected Topics in Power Electronics*, vol. 6, no. 3, pp. 1008–1020, 2018.

[20] S. Mohsenzade, M. Zarghany, and S. Kaboli, "A series IGBT switch with robustness against short-circuit fault for pulsed power applications," *IEEE Transactions on Power Electronics*, vol. 33, no. 5, pp. 3779–3790, 2018.

[21] L. V. Strezoski, M. D. Prica, V. A. Katic, and B. Dumnic, "Short-circuit modeling of inverter based distributed generators considering the FRT requirements," in *Proceedings of the 2016 North American Power Symposium (NAPS)*, Denver, CO, USA, September 2016.

[22] B. Lu and S. K. Sharma, "A literature review of IGBT fault diagnostic and protection methods for power inverters," *IEEE Transactions on Industry Applications*, vol. 45, no. 5, pp. 1770–1777, 2009.

[23] F. Huang and F. Flett, "IGBT fault protection based on *di*/*dt* feedback control," in *Proceedings of the IEEE 38th Annual Power Electronics Specialists Conference*, pp. 1478–1484, Piscataway, NJ, USA, September 2007.

[24] K. Rothenhagen and F. W. Fuchs, "Performance of diagnosis methods for IGBT open circuit faults in three phase voltage source inverters for AC variable speed drives," in *Proceedings of the European Conference of Power Electronics and Applications*, pp. 1–10, Dresden, Germany, September 2005.

[25] K. Rothenhagen and F. W. Fuchs, "Performance of diagnosis methods for IGBT open circuit faults in voltage source active rectifiers," in *Proceedings of the 2014 IEEE 35th Annual Power Electronics Specialists Conference*, pp. 4348–4354, Aachen, Germany, June 2004.

[26] A. Bhalla, S. Shekhawat, J. Gladish, J. Yedinak, and G. Dolny, "IGBT behavior during desat detection and short circuit fault protection," in *Proceedings of the International Symposium on Power Semiconductor Devices and IC's*, pp. 245–248, Kyoto, Japan, June 1998.

[27] R. S. Chokhawala and S. Sobhani, "Switching voltage transient protection schemes for high-current IGBT modules," *IEEE Transactions on Industry Applications*, vol. 33, no. 6, pp. 1601–1610, 1997.

[28] Robert Bosch GMBH, *Device and Method for Operating an Electric Machine: Germany*, Robert Bosch GMBH, Gerlingen, Germany, PCT/EP2014/074588, 2014.